Light-induced disassembly of self-assembled vesicle-capped nanotubes observed in real time

Coleman, Anthony C.; Beierle, John M.; Stuart, Marcus; Macia, Beatriz; Caroli, Giuseppe; Mika, Jacek T.; van Dijken, Derk Jan; Chen, Jiawen; Browne, Wesley; Feringa, B.L.

Published in:
Nature Nanotechnology

DOI:
10.1038/NNANO.2011.120

Publication date:
2011

nature nanotechnology

SUPPLEMENTARY INFORMATION

DOI: 10.1038/NNANO.2011.120

Light-induced disassembly of self-assembled vesicle-capped nanotubes observed in real-time

Anthony C. Coleman, John M. Beierle, Marc C. A. Stuart, Beatriz Maciá, Giuseppe Caroli, Jacek T. Mika, Derk Jan van Dijken, Jiawen Chen, Wesley R. Browne, Ben L. Feringa*

1. Materials and methods

Materials. Chemicals were purchased from Acros, Aldrich, Fluka or Merck. Solvents for extraction and chromatography were of technical grade. All solvents used in reactions were freshly distilled from appropriate drying agents before use. All other reagents were recrystallized or distilled as necessary. Analytical TLC was performed with Merck silica gel 60 F254 plates and visualization was accomplished by UV light. Flash chromatography was carried out using Merck silica gel 60 (230-400 mesh ASTM). Components were visualized by staining with a solution of a mixture of phosphomolibdic acid (4 g) in EtOH (80 mL). NMR spectra were obtained using a Varian Mercury Plus and a Varian Unity Plus Varian-500, operating at 199.97, 299.97, 399.93 and 499.86 MHz, respectively, for the ^{1}H nucleus or at 50.29, 75.5, 100.57 and 125.70 MHz, respectively, for the ^{13}C nucleus. Chemical shifts are reported in δ = units (ppm) relative to the residual protonated solvent signals of $CDCl_3$ (^{1}H NMR: δ = 7.26 ppm), DMSO-d_6 (^{1}H NMR: δ = 2.49 ppm), CD_2Cl_2 (^{1}H NMR: δ = 5.32 ppm) or at the carbon absorption in $CDCl_3$ (^{13}C NMR: δ = 77.0 ppm), DMSO-d_6 (^{13}C NMR: δ = 39.5 ppm) or CD_2Cl_2 (^{13}C NMR: δ = 53.8 ppm). Data are reported as follows: chemical shifts, multiplicity (s = singlet, d = doublet, t = triplet, q = quartet, br = broad, m = multiplet), coupling constants (Hz), and integration. MS (EI) spectra were obtained with a Jeol JMS-600 spectrometer.

Methods. *UV–Vis spectra* were recorded using a Jasco V-630 spectrophotometer in Uvasol grade solvents (Merck). Fluorescence spectra were recorded using a Jasco FP-6200 spectrofluorimeter in 1 mm pathlength quartz fluorescence cuvettes (Hellma). Low temperature UV-Vis studies were carried out on a Hewlett Packard 8453 Diode Array spectrophotometer fitted with a temperature controlled cell. Low temperatures were reached using a polystat CC1 cryostat with a Quantum Northwest temperature controller. Irradiation was carried out at an excitation wavelength of 365 nm using a Spectroline E-Series Hand-held UV lamp. Infrared spectra were measured using a Perkin Elmer Spectrum 400 spectrophotometer complete with an ATR attachment. The amphiphile **1** was measured as a solid applied directly to the ATR crystal. The nanotubes were

measured by first applying drops of an aqueous suspension of the nanotubes to the ATR crystal and allowing to dry in air.

Molecular models were generated using the Hyperchem 7.5 package[1]. The structures were optimized with the AMBER3 force field, as implemented therein. The PEG moieties were omitted from the calculations to reduce calculations times.

Samples for cryo-TEM were prepared by depositing a few μL of vesicle solution on holey carbon coated grids (Quantifoil 3.5/1, Quantifoil Micro Tools, Jena, Germany). After blotting the excess liquid, the grids were vitrified in liquid ethane (Vitrobot, FEI, Eindhoven, The Netherlands) and transferred to a Philips CM 120 cryo-electron microscope equipped with a Gatan model 626 cryo-stage operating at 120 kV. Micrographs were recorded under low-dose conditions with a slow-scan CCD camera. The bilayer thickness was measured on slightly defocused cryo-electron microscopy images to obtain maximal phase contrast. The highest density is obtained from the electron dense overcrowded alkene part of the amphiphile[2].

Differential Scanning Calorimetry (DSC) was measured using a Perkin Elmer DSC 7 equipped with a thermal analysis controller TAC71DX connected to a PC with Pyris Series DSC-7 software.

Nanotube suspensions for degradation studies were irradiated with a 400.8 nm CW laser (Power Technology, Arkansas, USA).

Microscopy studies of nanotubes for the experiments described in Figure 3e-f and 4a-i were carried out with an Andor DSD Confocal microscope system. Filters used in the experiments described in Figure 3b and 4e-h, median wavelength = 406 nm, bandwidth = 15 nm and median wavelength = 494 nm, bandwidth = 20 nm. Epifluorescence analysis was carried out using a Nikon Illuminator CoolLED system with Semrock Filters: LF405-A-NTE (median wavelength = 390 nm, bandwidth = 40 nm) and LF488-A-NTE (median wavelength 482 nm, bandwidth = 18 nm).

Wide field imaging of tubes and vesicles for the experiment detailed in Figure S6 was carried out on a Zeiss Observer Z1 microscope equipped with a 63 x water immersion l objective (Zeiss plan-neoFluar), a Colibri LED excitation source and a Cool-Snap HQ CCD camera (Photometrics, Tucson, AZ, USA). For the imaging of the DIO labelled tubes (green channel) 505 and 470 nm LED excitiation was used and emission

was detected between 520 and 550 nm, while the DID labelled (red channel) vesicles were excited with a 625 nm LED and emission was collected between 662 and 715 nm. The green and red channel images were overlaid using AxioVision40 software V 4.8.2.0 from Zeiss Microimaging GmbH.

Standard method for tube formation: Amphiphile **1** was mixed with the desired amount of DOPC in chloroform and subsequently dried under nitrogen gas followed by further solvent removal under high vacuum for one hour. After hydration in water the suspension was subjected to five freeze-thaw cycles to form end-capped tubes. Freezing breaks up the vesicle structure as a result of ice crystal formation. Upon thawing the exposed hydrophobic surfaces reseal on each other, thus reforming the vesicles, while some vesicles reseal on the hydrophobic ends of the amphiphilic tubes. When low amounts of detergents such as Triton X-100 are present the hydrophobic tube ends are likely covered with detergent molecules thereby impeding vesicle reattachment. Only when all the detergent has been removed can the vesicles be reattached by freeze-thaw cycles[3].

2. Synthesis

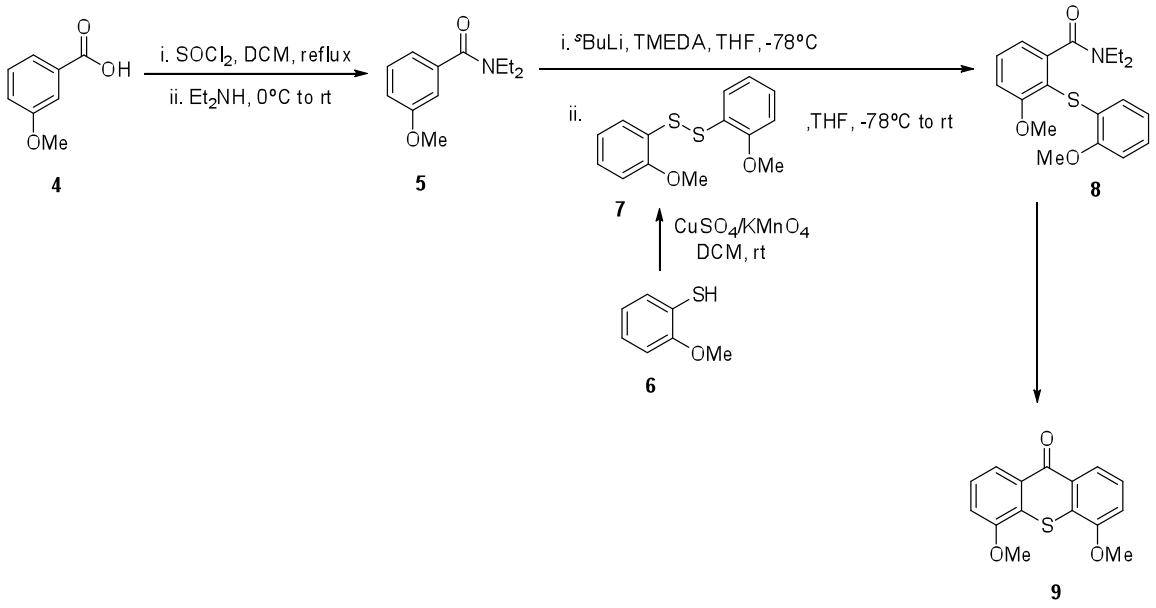

Scheme S1

4,5-Dimethoxy-9*H*-thioxanthen-9-one (**9**) was prepared according to the previously reported synthetic route depicted in Scheme 1. Experimental data of **9** is in accordance with that reported[4].

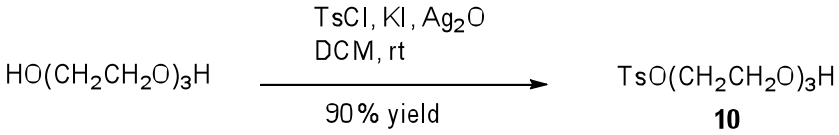

Scheme S2

2-(2-(2-Hydroxythoxy)ethoxy)ethyl 4-methylbenzenesulfonate (10) was prepared from triethyleneglycol following literature procedures. Experimental data of **10** is in accordance with that reported[5].

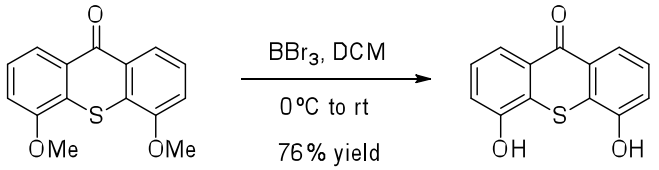

9 **11**

Scheme S3

4,5-Dihydroxy-9*H*-thioxanthen-9-one (11): compound **9** (600 mg, 2.20 mmol) was dissolved in dry dichloromethane (200 mL) under a nitrogen atmosphere and 5 equivalents of boron tribromide were slowly added at 0 °C. The mixture was allowed to reach room temperature while stirring overnight. After warming the reaction mixture to 0 °C, cold water (50 mL) was slowly added. The aqueous layer was extracted five times with EtOAc and the solvent removed under vacuum to yield **11** as green solid (410 mg, 76 %); m.p. not determinable (decomposition).

^{1}H NMR (300 MHz, DMSO): δ 10.98 (s, 2H, OH); 7.94 (d, J = 7.7 Hz, 2H); 7.38 (dd, J = 7.7, 7.7 Hz, 2H); 7.20 (d, J =7.7 Hz, 2H); ^{13}C NMR (50 MHz, DMSO): δ 180.0; 153.7; 130.0; 127.0; 126.0; 119.9; 117.2; HRMS (APCI positive): calcd. for $C_{13}H_9O_3S$ (M^+ + H): 245.0267, found 245.0259.

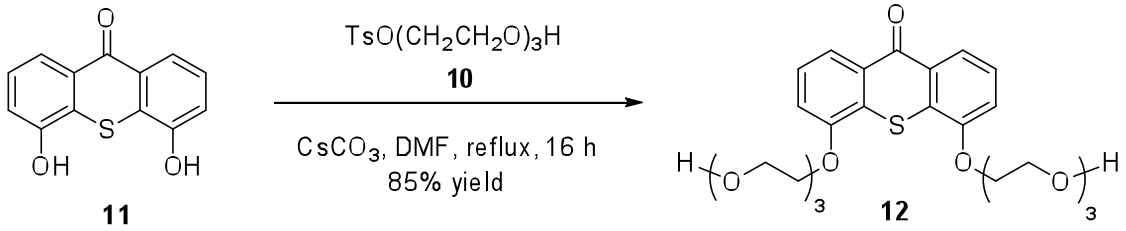

11 **12**

Scheme S4

4,5-Bis(2-(2-(2-hydroxyethoxy)ethoxy)ethoxy)-9H-thioxanten-9-one (12): compound **11** (244 mg, 1.0 mmol) was dissolved in dry DMF (30 mL). $CsCO_3$ (1.6 g, 5.0 mmol) and compound **10** (639 mg, 2.1 mmol) was added and the mixture heated at reflux 16 h under nitrogen atmosphere. After cooling to room temperature, the reaction mixture was filtered over celite and the celite cake washed with EtOAc and DCM. The solvents were removed

by rotary evaporation and the residue purified by column chromatography (CH_2Cl_2: MeOH, 20:1) to yield **12** as a yellow solid (432 mg, 85 % yield); m.p. 36 ^oC

^1H NMR (400 MHz, $CDCl_3$) δ = 8.18 (dd, *J* = 8.2, 1.1 Hz, 2H), 7.36 (td, *J* = 8.1, 1.0 Hz, 2H), 7.10 (d, *J* = 8.0 Hz, 2H), 4.34 – 4.26 (t, *J* = 5.1 Hz, 4H), 3.95 (t, *J* = 5.1 Hz, 4H), 3.84 – 3.75 (m, 4H), 3.72 – 3.65 (m, 8H), 3.63 – 3.52 (m, 4H), 3.14 (s, 2H); ^{13}C NMR (101 MHz, $CDCl_3$) δ = 180.0, 153.9, 129.8, 127.9, 125.8, 121.6, 113.4, 72.6, 72.5, 71.0, 70.3, 70.1, 69.3, 69.1, 61.5; HRMS (APCI positive): calcd. for $C_{25}H_{33}O_9S$ (M^+ + H): 509.1839, found 509.1818.

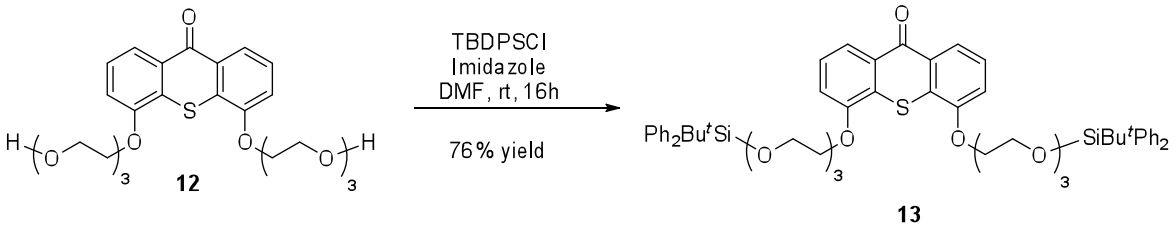

Scheme S5

4,5-Bis(2,2-dimethyl-3,3-diphenyl-4,7,10-trioxa-3-siladodecan-12-yloxy)-9*H*-thioxanthen-9-one (13): Compound **12** (390 mg, 0.77 mmol) was dissolved in dry DMF (20 mL) and TBDPSCl (541 mg, 2.00 mmol) and imidazole (159 mg, 2.30 mmol) were added at 0 ^oC. The reaction mixture was stirred 16 h at room temperature. The solvent was removed by rotary evaporation and **13** was obtained after column chromatography (Pentane:EtOAc, 1:1) as a yellow viscous oil (571 mg, 76 % yield).

^1H NMR (300 MHz, $CDCl_3$) δ = 8.23 (d, *J* = 8.0 Hz, 2H), 7.76 – 7.62 (m, 10H), 7.43 – 7.29 (m, 10H), 7.13 (d, *J* = 7.9 Hz, 2H), 4.30 (t, *J* = 4.9 Hz, 4H), 3.95 (t, *J* = 4.9 Hz, 4H), 3.86 – 3.57 (m, 16H), 1.03 (s, 18H); ^{13}C NMR (75 MHz, $CDCl_3$) δ = 180.4, 154.4, 135.8, 133.9, 130.2, 129.9, 128.4, 127.9, 126.1, 121.9, 113.9, 72.7, 71.4, 71.1, 69.8, 69.5, 63.7, 27.1, 19.4; HRMS (ESI negative): calcd. for $C_{57}H_{68}O_9SSi_2Cl$ (M^+ + Cl): 1019.3805, found 1019.3780.

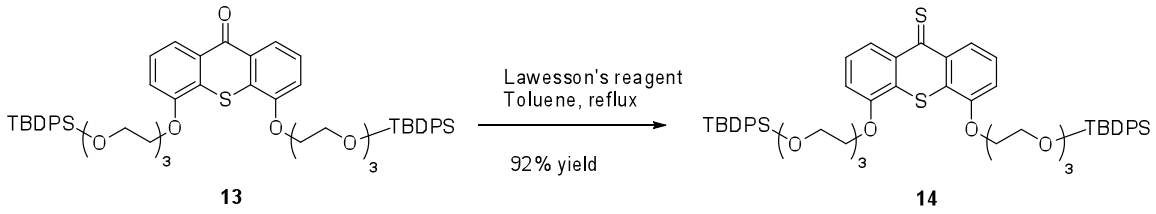

Scheme S6

4,5-Bis(2,2-dimethyl-3,3-diphenyl-4,7,10-trioxa-3-siladodecan-12-yloxy)-9*H*-thioxanthene-9-thione (14): Compound **13** (540 mg, 0.55 mmol) was dissolved in dry toluene (20 mL) and Lawesson's reagent (685 mg, 1.65 mmol) was added. The reaction mixture was heated at 90 ^{o}C for 7 h. The solvent was removed by rotary evaporation and the crude material was purified by column chromatography (EtOAc:Pentane, 2:1) to yield **14** as a viscous green oil (505 mg, 92 %); ^{1}H NMR (400 MHz, $CDCl_3$) δ = 8.67 (d, *J* = 8.4 Hz, 2H), 7.70 – 7.66 (m, 10H), 7.42 – 7.31 (m, 14H), 7.14 (d, *J* = 7.9 Hz, 2H), 4.33 (t, *J* = 5.0 Hz, 4H), 3.97 (t, *J* = 5.0 Hz, 4H), 3.82 (t, *J* = 5.3 Hz, 4H), 3.77 – 3.73 (m, 4H), 3.72 - 3.65 (m, 4H), 3.62 (t, *J* = 5.3 Hz, 4H), 1.04 (s, 18H); ^{13}C NMR (101 MHz, $CDCl_3$) δ = 210.7, 154.2, 138.3, 135.6, 133.6, 129.6, 127.6, 126.3, 125.6, 112.8, 72.5, 71.2, 70.9, 69.5, 69.4, 63.4, 26.8, 19.2; HRMS (APCI positive): calcd. for $C_{57}H_{69}O_8S_2Si_2$ (M^+ + H): 1001.3967, found 1001.3911.

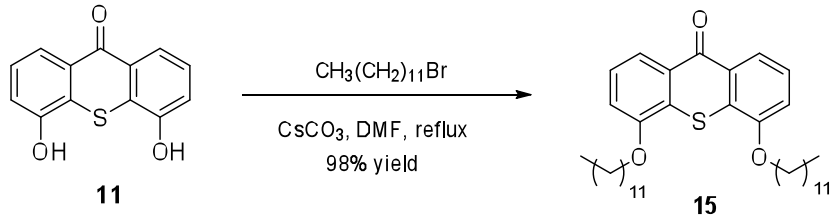

Scheme S7

4,5-Bis(dodecyloxy)-9*H*-thioxanthen-9-one (15): compound **11** (200 mg, 0.82 mmol) was dissolved in dry DMF (30 mL). $CsCO_3$ (1.3 g, 4.10 mmol) and dodecyl bromide (425 μL, 2.10 mmol) were added and the mixture heated at reflux for 16 h under nitrogen atmosphere. After cooling down to room temperature, the reaction mixture was filtered over celite and the celite cake washed with EtOAc and DCM. The solvents were removed

by rotary evaporation and the residue purified by column chromatography (EtOAc: Pentane, 1:5) to yield **15** as a yellow solid (464 mg, 98 % yield); m.p. 78 ^{o}C.

^{1}H NMR (400 MHz, $CDCl_3$) δ = 8.23 (dd, *J* = 8.1, 1.2 Hz, 2H), 7.41 (td, *J* = 8.1, 1.4 Hz, 2H), 7.12 (d, *J* = 8.0 Hz, 2H), 4.18 (t, *J* = 6.4 Hz, 4H), 2.00 – 1.85 (m, 4H), 1.65 – 1.55 (m, 4H), 1.44 – 1.20 (m, 16H), 0.87 (m, 6H); ^{13}C NMR (101 MHz, $CDCl_3$) δ = 180.4, 154.4, 130.0, 128.4, 125.8, 121.2, 113.0, 69.4, 31.9, 29.7, 29.6, 29.3, 29.0, 26.0, 22.7, 14.1. HRMS (APCI positive): calcd. for $C_{37}H_{57}O_3S$ (M^+ + H): 581.4023, found 581.4002.

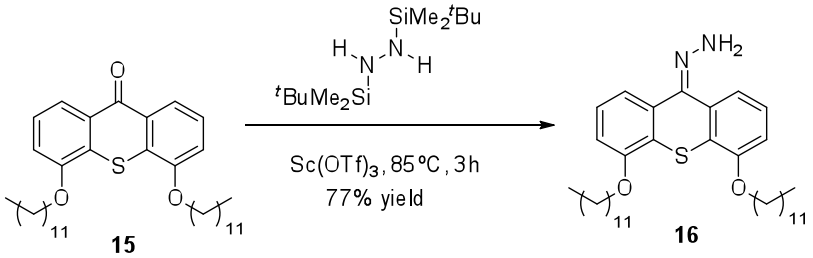

Scheme S8

(4,5-Bis(dodecyloxy)-9*H*-thioxanthen-9-ylidene)hydrazine (16): $Sc(OTf)_3$ (0.1 mol%) and TBDMS-protected hydrazine[6] (166 mg, 0.64 mmol) were added to compound **15** (185 mg, 0.32 mmol) at 0 ^{o}C under a nitrogen atmosphere. The mixture was heated at 80 ^{o}C for 3 h. The excess of hydrazine was evaporated under high vacuum at 100 ^{o}C and the final residue purified by column chromatography (pentane:EtOAc, 15:5) to yield **16** as a yellow solid (146 mg, 77 % yield), m.p. 81 ^{o}C.

^{1}H NMR (300 MHz, $CDCl_3$) δ = 7.63 (d, *J* = 7.8 Hz, 1H), 7.43 (d, *J* = 7.8 Hz, 1H), 7.25 (m, 2H), 6.87 (d, *J* = 8.1 Hz, 1H), 6.82 (d, *J* = 7.9 Hz, 1H), 5.84 (s, 2H), 4.08 (dd, *J* = 14.2, 6.7 Hz, 4H), 1.88 (dd, *J* = 13.8, 6.9 Hz, 4H), 1.55 (m, 4H), 1.35 (m, 20H), 0.87 (t, *J* = 7.6 Hz, 6H); ^{13}C NMR (75 MHz, $CDCl_3$) δ = 155.9, 154.3, 142.0, 135.3, 127.0, 126.7, 125.7, 121.8, 120.1, 118.4, 111.2, 110.2, 69.4, 32.2, 29.9, 29.6, 29.4, 26.3, 22.9, 14.4; HRMS (APCI positive): calcd. for $C_{37}H_{59}N_2O_2S$ (M^+ + H): 595.4292, found 595.4266.

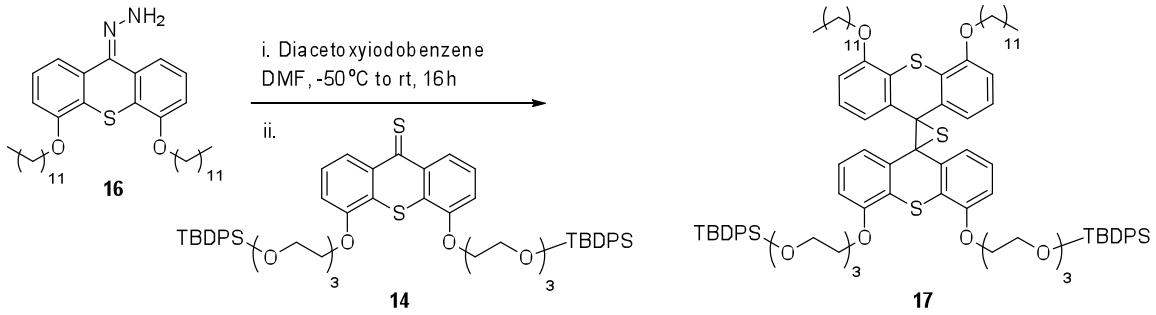

Scheme S9

Episulfide 17: Hydrazone **16** (89 mg, 0.15 mmol) was dissolved in dry DMF (5 mL) and, placed under a nitrogen atmosphere, the mixture was cooled to -50 °C. Diacetoxyiodobenzene (49 mg, 0.15 mmol) dissolved in DMF (2 mL) was added dropwise and the mixture stirred for 5 min at the same temperature. Thioketone **14** (150 mg, 0.15 mmol) dissolved in DMF (5 mL) was added slowly and the reaction mixture was stirred for 16 h at room temperature. After filtration over celite, the solvent was removed by rotary evaporation and the residue was purified by column chromatography (pentane:EtOAc, 3:1) to provide the corresponding episulfide **17** (54 mg, 23 % yield).

^{1}H NMR (400 MHz, $CDCl_3$) δ = 7.70 (d, *J* = 6.7 Hz, 10H), 7.40 – 7.33 (m, 12H), 7.32 (d, *J* = 7.9 Hz, 2H), 7.28 (d, *J* = 7.8 Hz, 2H), 6.85 (dd, *J* = 10.5, 5.4 Hz, 4H), 6.56 (d, *J* = 7.9 Hz, 2H), 6.51 (d, *J* = 8.0 Hz, 2H), 4.15 – 4.03 (m, 4H), 4.01 – 3.89 (m, 4H), 3.82 – 3.70 (m, 10H), 3.65 – 3.60 (m, 10H), 1.91 – 1.66 (m, 2H), 1.28 (m, 4H), 1.07 (s, 34H), 0.90 (t, *J* = 6.1 Hz, 6H); ^{13}C NMR (101 MHz, $CDCl_3$) δ = 154.1, 153.8, 135.8, 133.9, 132.6, 132.1, 129.8, 127.9, 126.0, 125.7, 125.2, 125.0, 124.0, 123.3, 120.1, 118.4, 111.6, 111.2, 110.3, 110.2, 72.7, 71.3, 71.0, 69.8, 69.5, 69.4, 63.6, 32.2, 30.0, 29.9, 29.8, 29.7, 29.6, 29.5, 29.4, 27.1, 26.3, 26.2, 23.0, 19.4, 14.4; HRMS (APCI negative): calcd. for $C_{94}H_{123}O_{10}S_3Si_2$: 1564.7845, found 1564.7883.

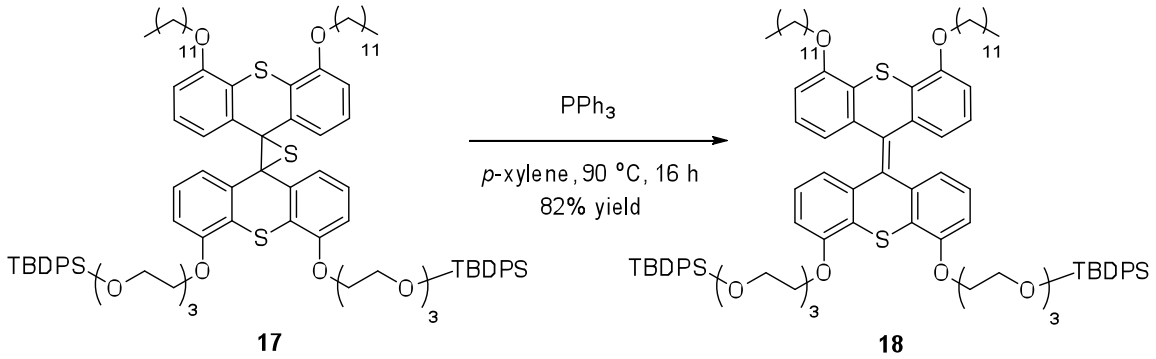

17 **18**

Scheme S10

Compound 18: Compound **17** (54 mg, 0.034 mmol) was dissolved in *p*-xylene (5 mL) and PPh_3 (48 mg, 0.17 mmol) was added. The reaction mixture was heated at 95 ^oC for 16 h. The solvent was removed by rotary evaporation followed by purification by column chromatography (pentane:EtOAc, 3:1) (43 mg, 82 % yield).

^1H NMR (400 MHz, $CDCl_3$) δ = 7.81 – 7.63 (m, 10H), 7.44 – 7.32 (m, 10H), 6.81 (t, *J* = 7.9 Hz, 4H), 6.67 (d, *J* = 5.1 Hz, 2H), 6.65 (d, *J* = 5.2 Hz, 2H), 6.44 (d, *J* = 7.8 Hz, 2H), 6.39 (d, *J* = 7.8 Hz, 2H), 4.36 – 4.25 (m, 2H), 4.15 (dt, *J* = 16.1, 5.6 Hz, 4H), 4.06 – 3.90 (m, 6H), 3.82 (m, 8H), 3.75 – 3.58 (m, 8H), 1.91 (m, 4H), 1.59 (m, 4H), 1.35 (m, 32H), 1.06 (s, 18H), 0.97 – 0.76 (m, 6H); ^{13}C NMR (101 MHz, $CDCl_3$) δ = 155.4, 155.1, 137.0, 136.6, 135.8, 133.9, 129.8, 127.9, 126.0, 125.9, 125.0, 122.8, 122.3, 109.6, 109.3, 72.7, 71.4, 71.1, 69.9, 69.2, 68.8, 63.6, 32.2, 30.0, 29.9, 29.8, 29.6, 29.5, 27.1, 26.4, 22.9, 19.4, 14.4; HRMS (ESI negative): calcd. for $C_{94}H_{123}O_{10}S_2Si_2Cl$ (M^+ - H + Cl): 1567.7813, found 1567.7879.

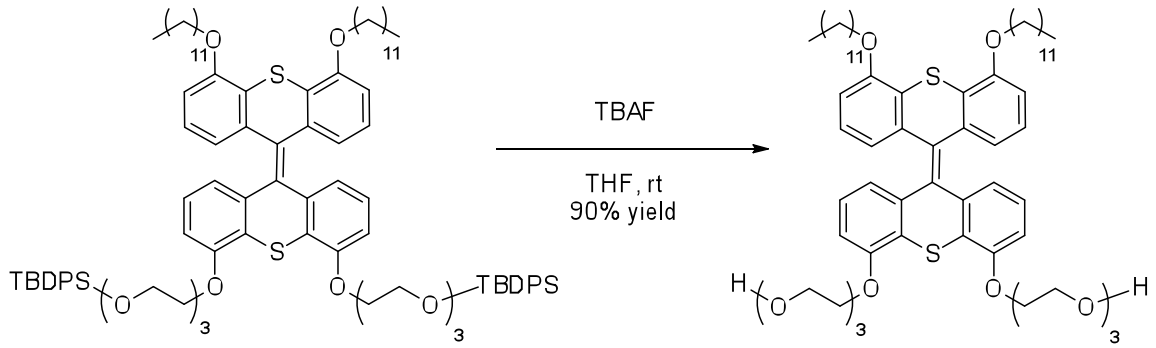

18 **1**

Scheme S11

Compound 1: Compound **18** (32 mg, 0.021 mmol) was dissolved in THF (1 mL) and TBAF (1 M in THF) (0.05 mL, 0.05 mmol) was added at 0 ^{o}C. The reaction mixture was stirred at room temperature for 16 h. The solvent was removed by rotary evaporation and the residue purified by column chromatography (EtOAc:MeOH, 10:1) and recrystallization (pentane/DCM) (20 mg, 90 % yield).

^{1}H NMR (400 MHz, $CDCl_3$) δ 6.82 (dd, *J* = 14.5, 7.8 Hz, 4H), 6.66 (t, *J* = 7.3 Hz, 4H), 6.44 (d, *J* = 7.7 Hz, 2H), 6.38 (d, *J* = 7.7 Hz, 2H), 4.31 (d, *J* = 4.4 Hz, 2H), 4.20 (d, *J* = 4.2 Hz, 2H), 4.13 (d, *J* = 9.0 Hz, 2H), 4.00 (dd, *J* = 9.5, 6.2 Hz, 6H), 3.90 (t, *J* = 4.6 Hz, 4H), 3.76 (d, *J* = 3.1 Hz, 8H), 3.70 – 3.63 (m, 4H), 2.95 (s, 1H), 1.96 – 1.85 (m, 4H), 1.70 (d, *J* = 2.8 Hz, 1H), 1.57 (dd, *J* = 13.9, 6.6 Hz, 4H), 1.43 – 1.21 (m, 32H), 0.88 (t, *J* = 6.7 Hz, 6H).^{13}C NMR (75 MHz, $CDCl_3$) δ = 155.4, 155.0, 137.2, 136.5, 133.5, 132.8, 126.1, 125.9, 125.0, 124.8, 122.9, 122.3, 118.7, 109.5, 109.3, 73.0, 71.4, 70.8, 69.9, 69.2, 69.0, 62.0, 32.2, 29.9, 29.7, 29.63, 29.5, 26.4, 22.9, 14.4; HRMS (APCI positive): calcd. for $C_{62}H_{89}O_{10}S_2$ (M^+ + H): 1057.5897, found 1057.5889.

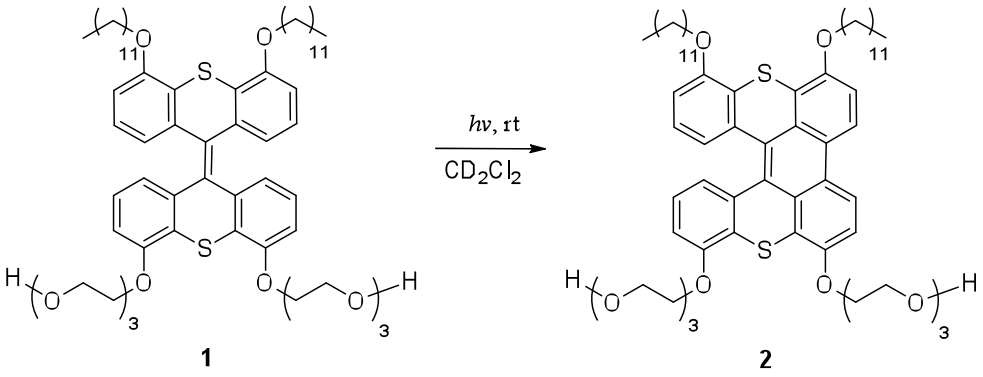

1 **2**

Scheme S12

Compound 2: Compound **1** (2 mg) was dissolved in CD_2Cl_2 (1 mL) in an NMR tube and the solution was irradiated (365 nm with a portable UV lamp) at room temperature for 2 h. This resulted in a change in the fluorescence of the sample from blue to green fluorescence.

^{1}H NMR (500 MHz, CD_2Cl_2) δ = 8.21 (d, *J* = 9.0 Hz, 2H), 7.26 (t, *J* = 9.0 Hz, 2H), 7.11 – 6.98 (m, 2H), 6.83 (dd, *J* = 13.2, 8.0 Hz, 2H), 6.77 – 6.70 (m, 2H), 4.45 – 4.38 (m, 2H), 4.36 – 4.05 (m, 6H), 4.06 – 4.96 (m, 4H), 3.92 - 3.82 (m, 4H), 3.79 – 3.70 (m, 8H), 3.66 (d, *J* = 3.9 Hz, 4H), 1.97 – 1.93 (m, 4H), 1.65 – 1.61 (m, 4H), 1.35 – 1.25 (m, 32H), 0.91 (t, *J* = 7.0 Hz, 6H).

HRMS (APCI positive): calcd. for $C_{62}H_{87}O_{10}S_2$ (M^+ + H): 1055.5735, found 1055.5709.

3. ^{1}H- and ^{13}C-NMR spectra

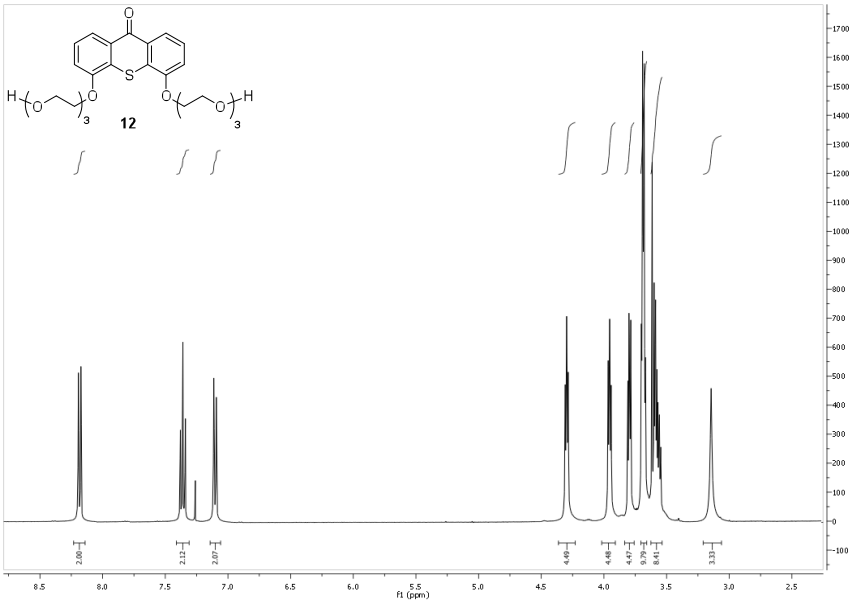

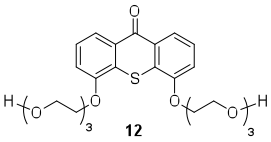

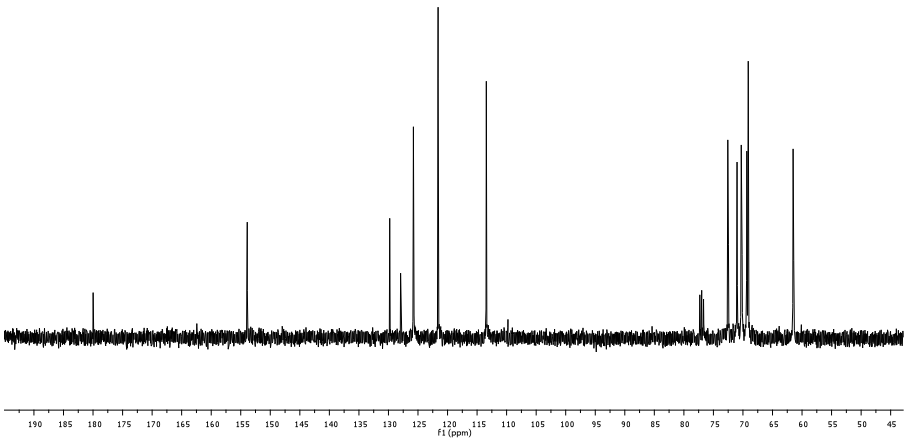

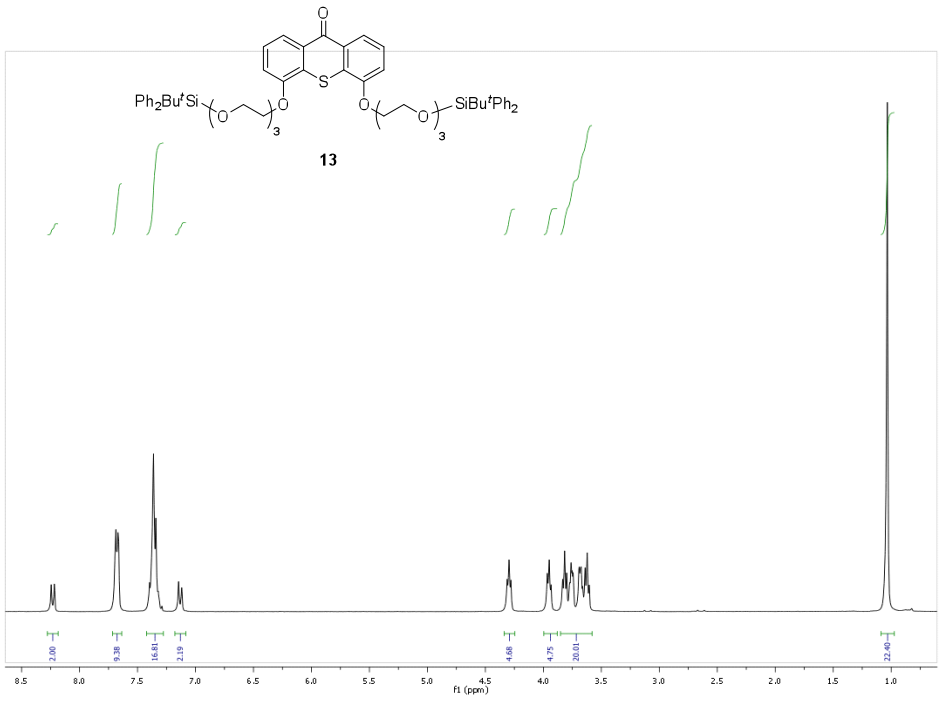

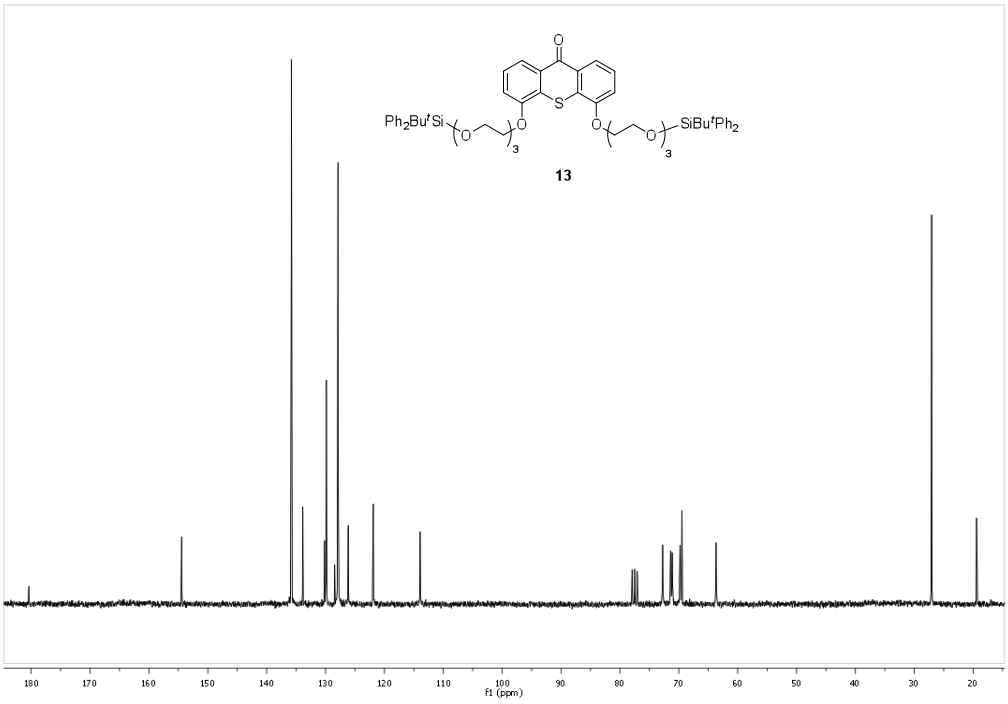

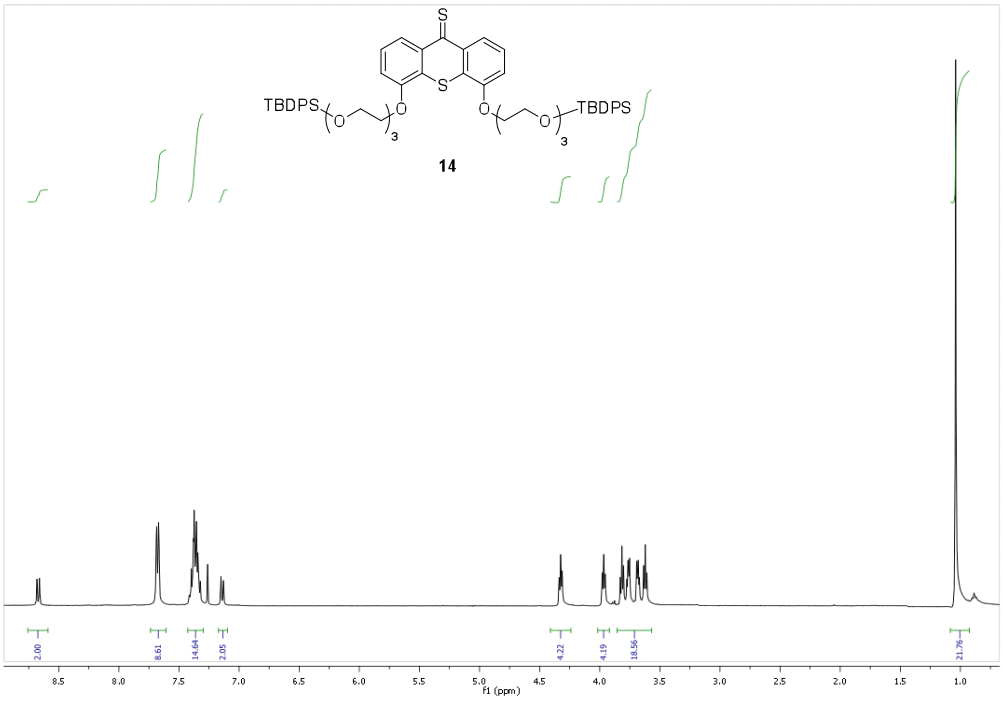

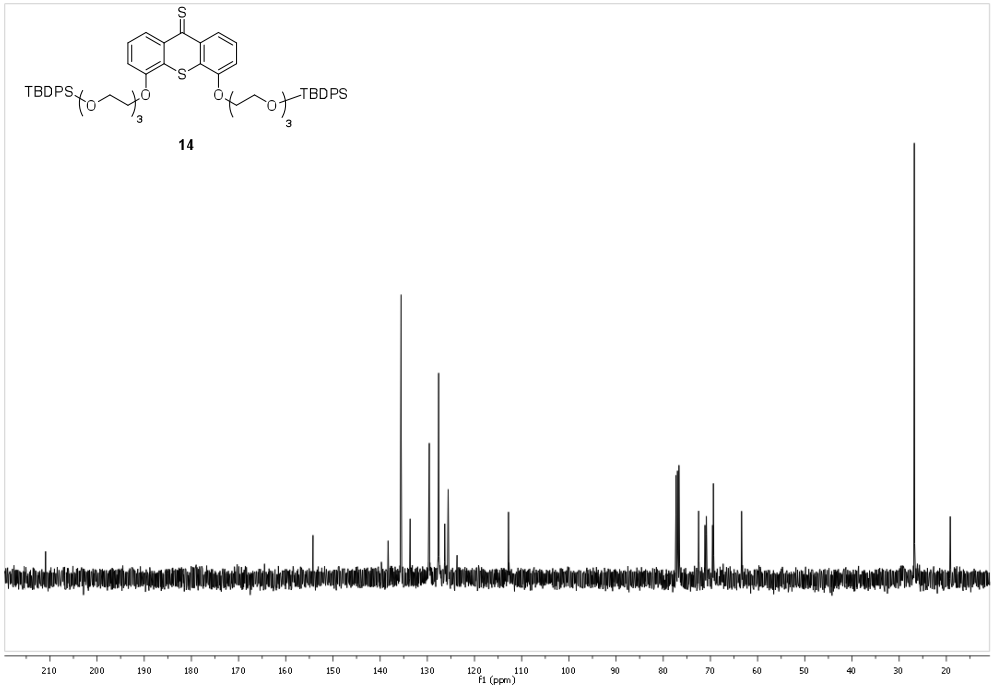

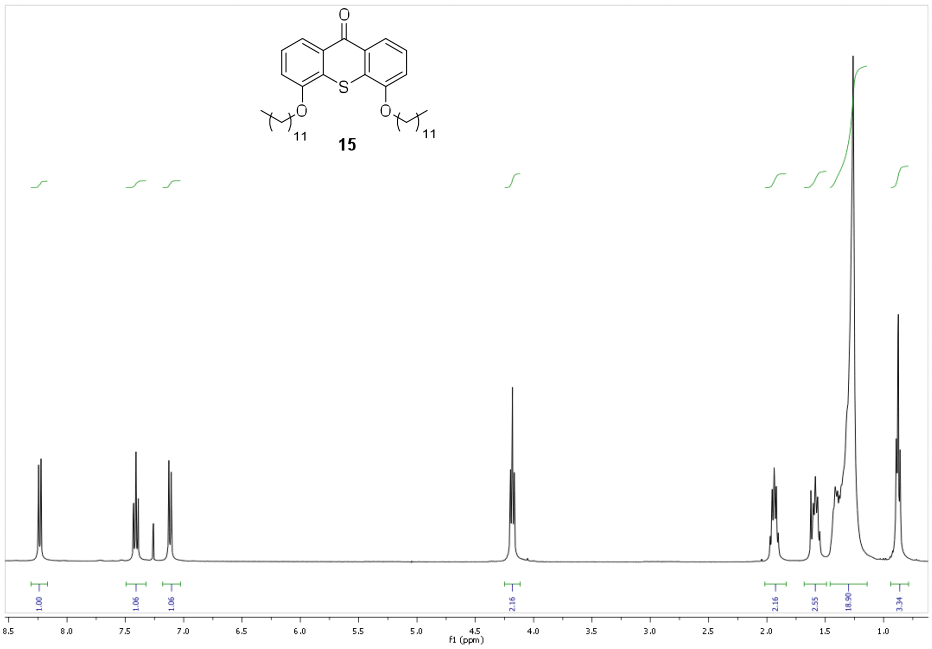

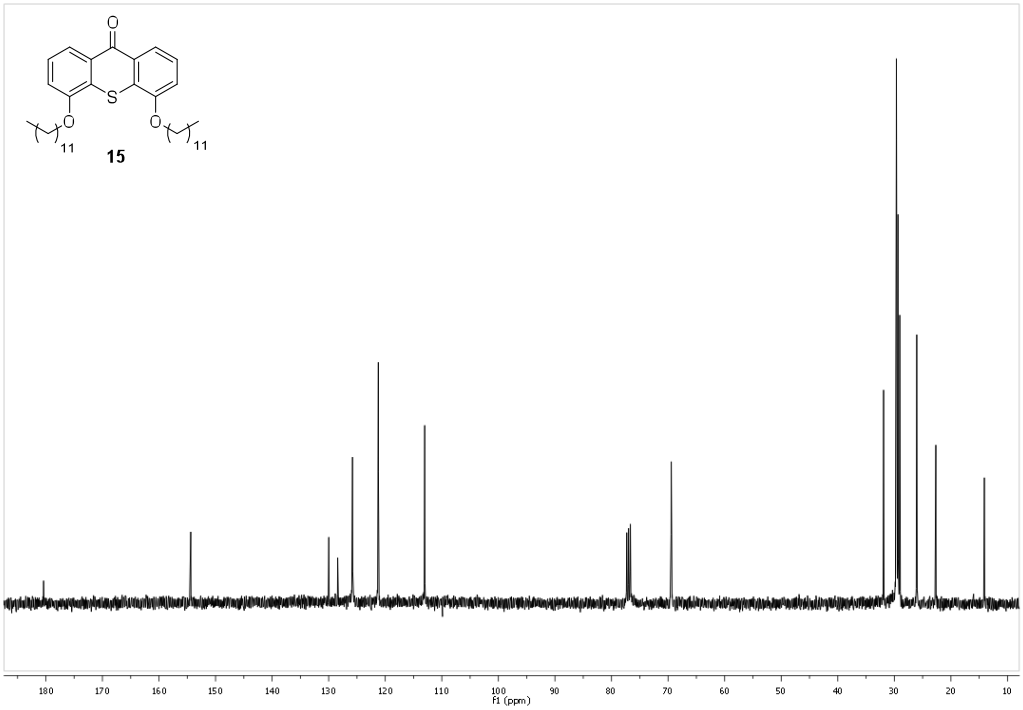

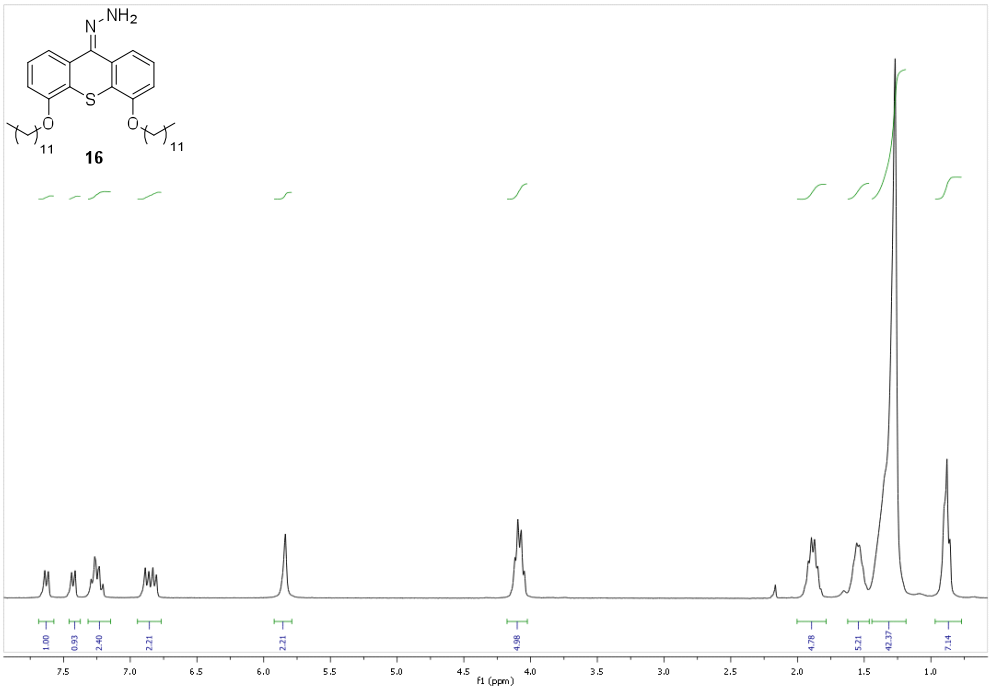

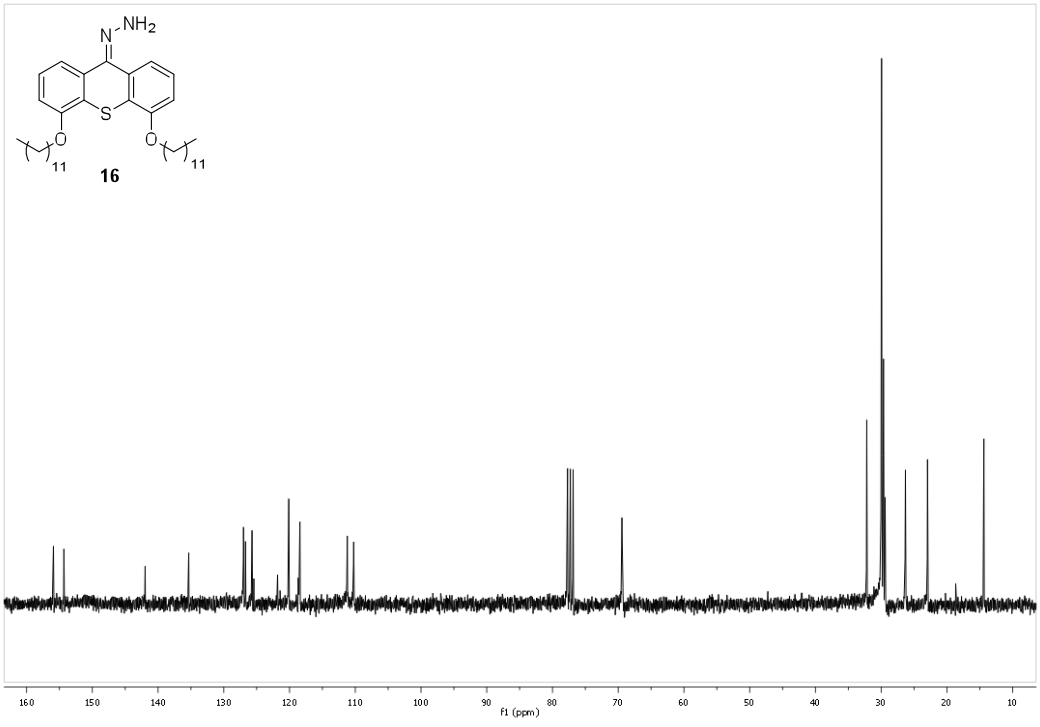

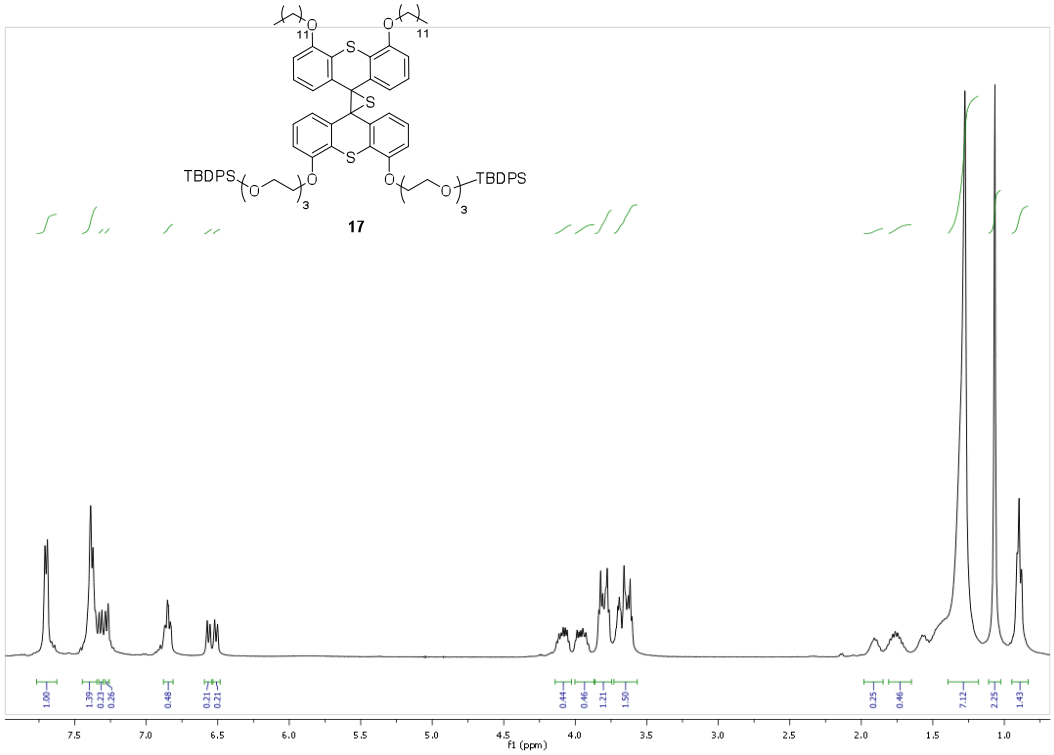

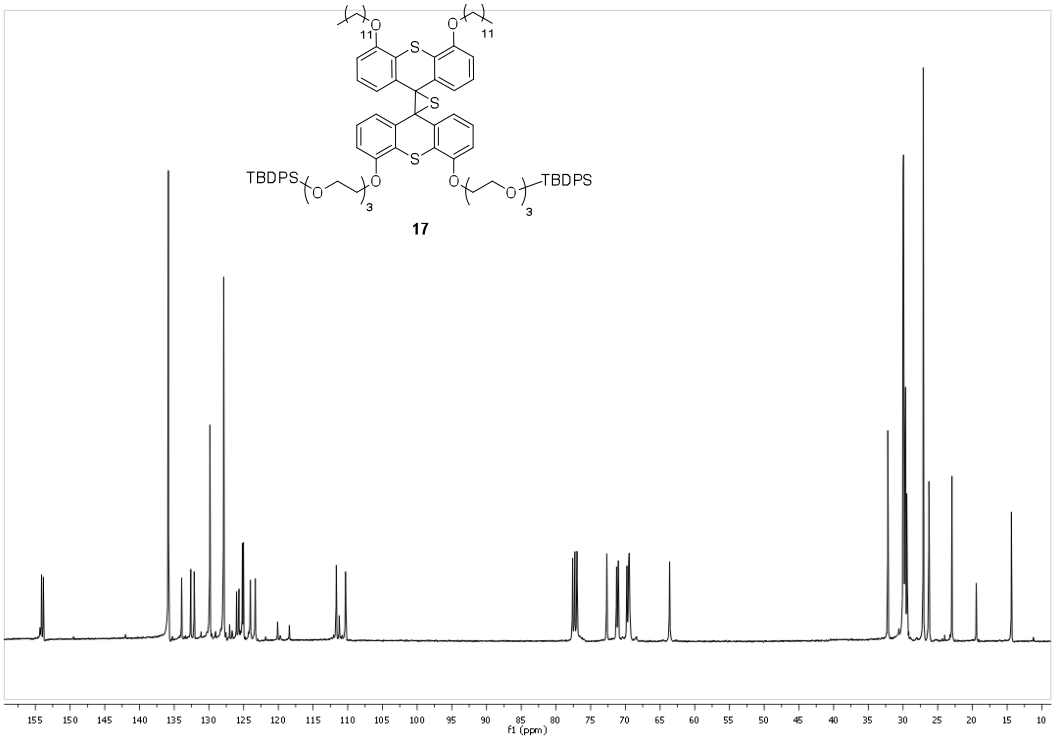

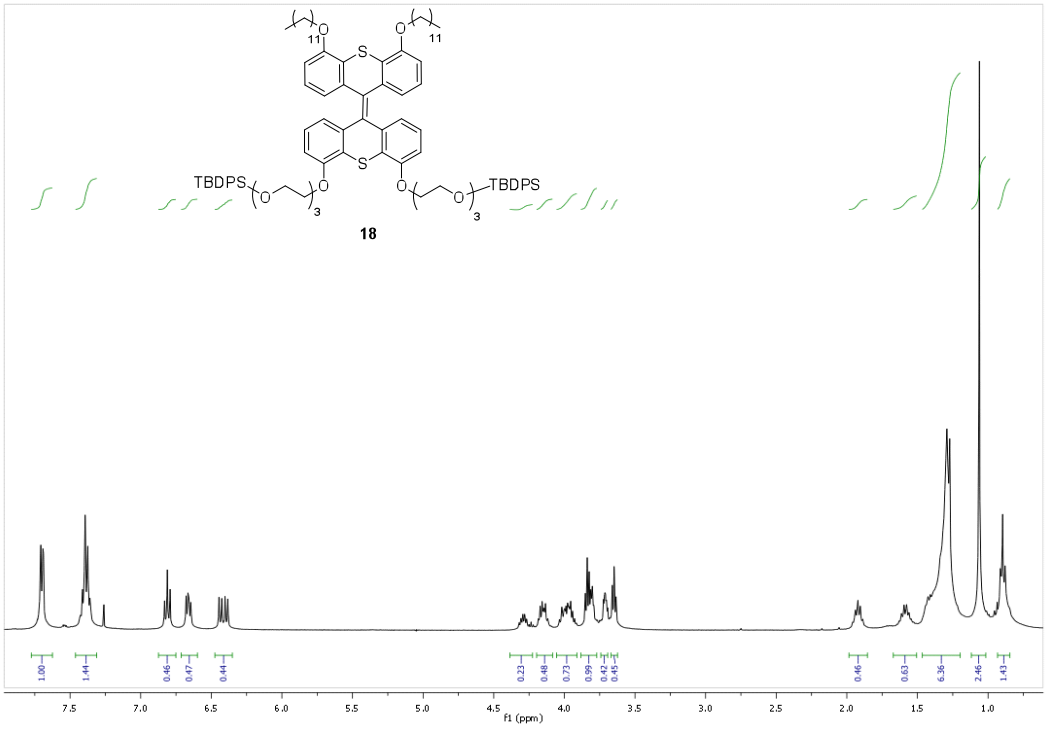

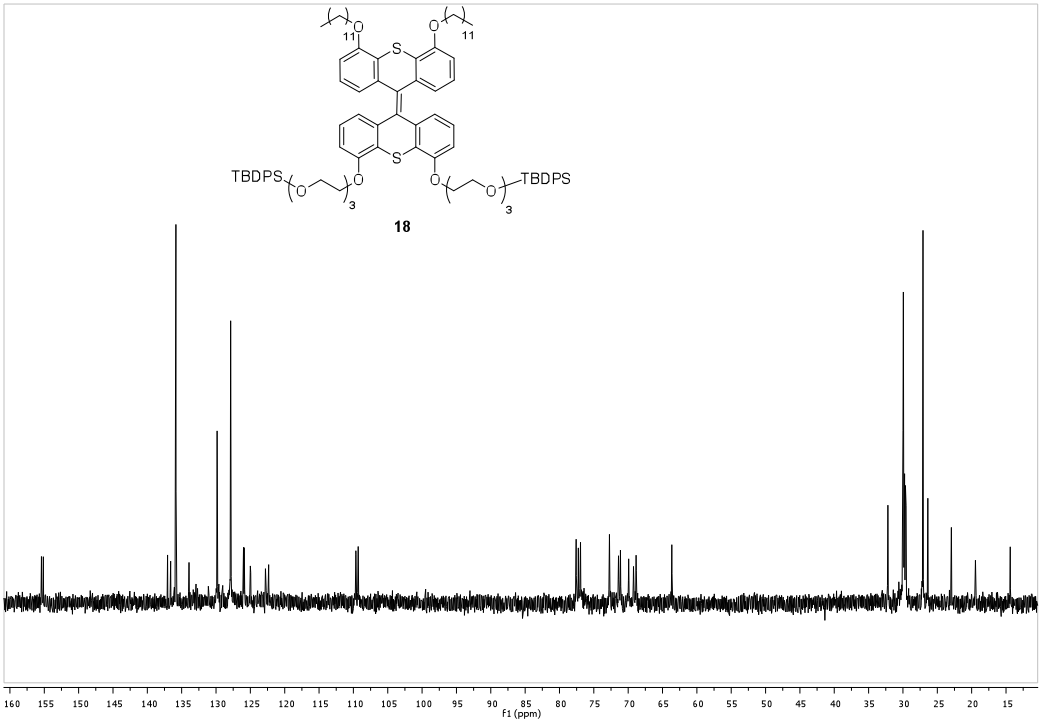

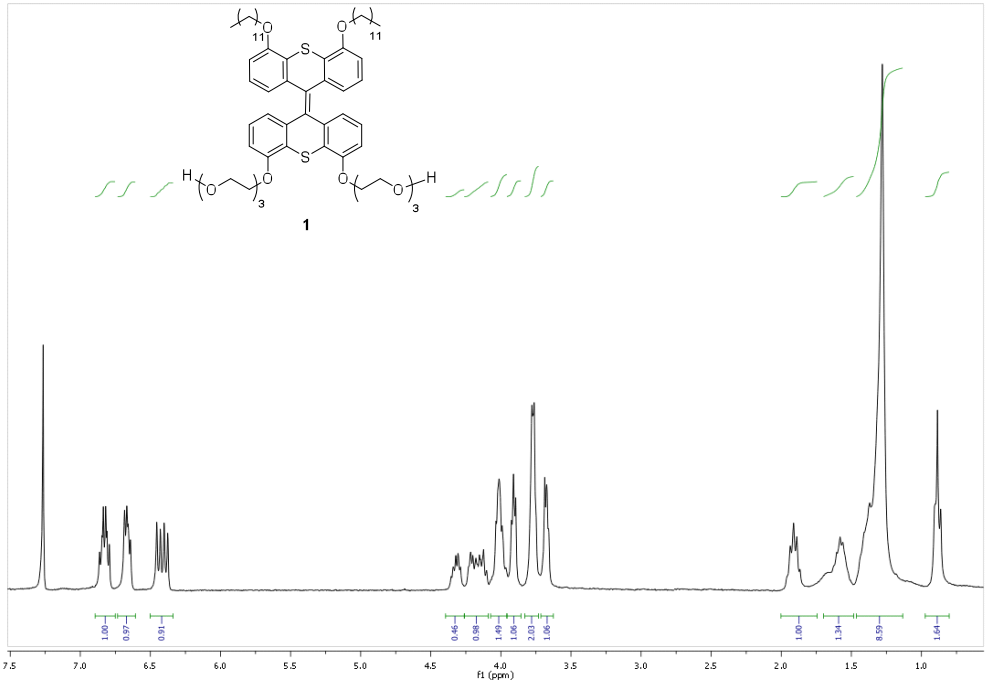

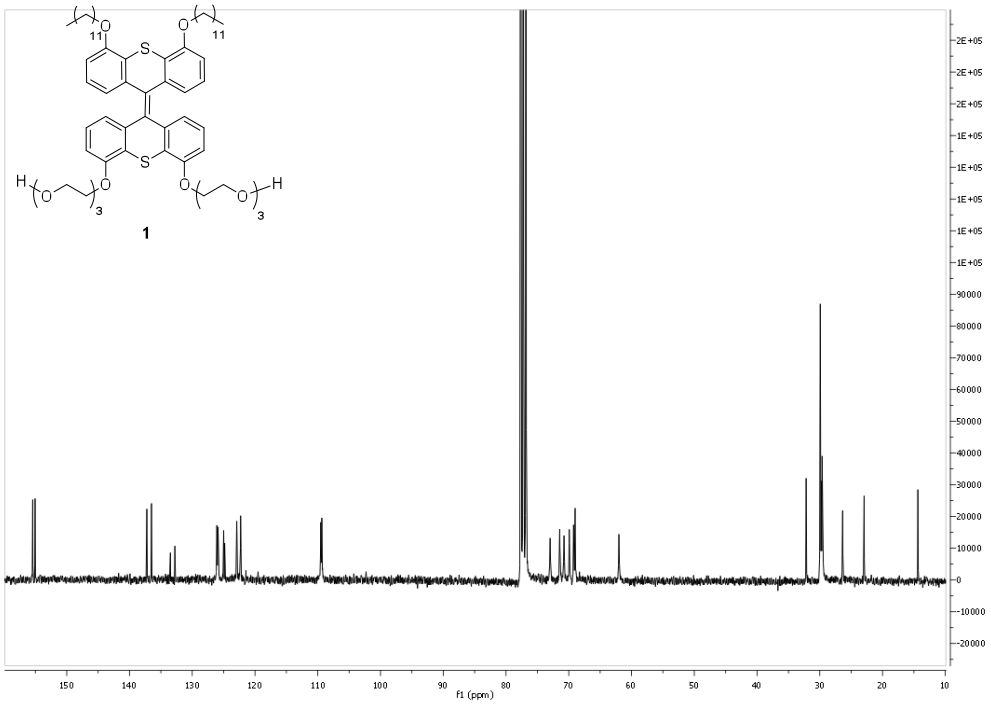

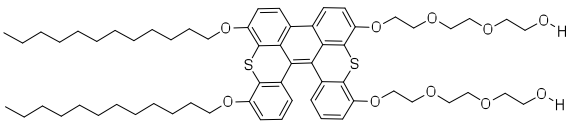

3

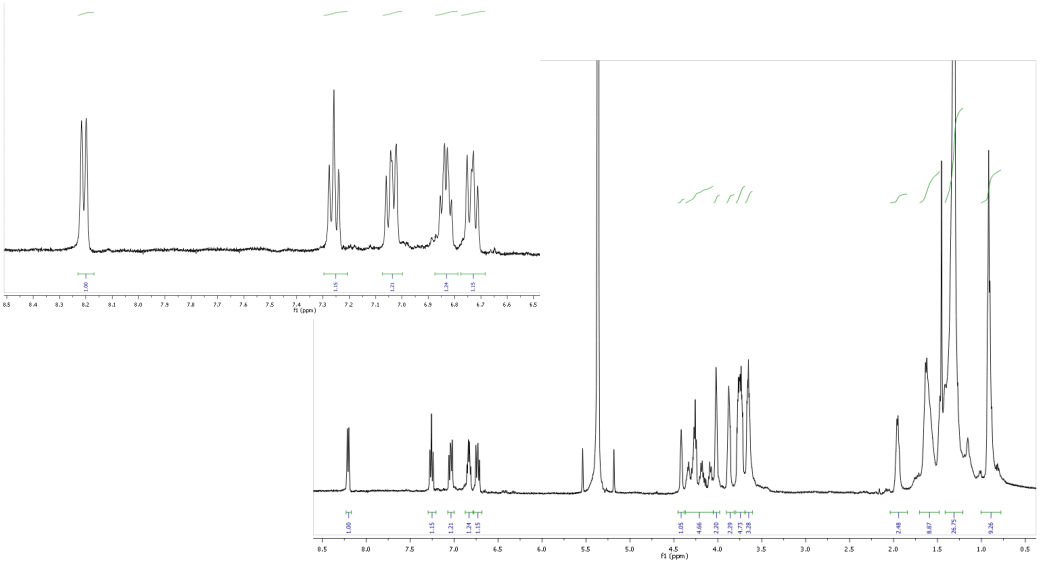

4. Amphiphile 1/DOPC ratio studies

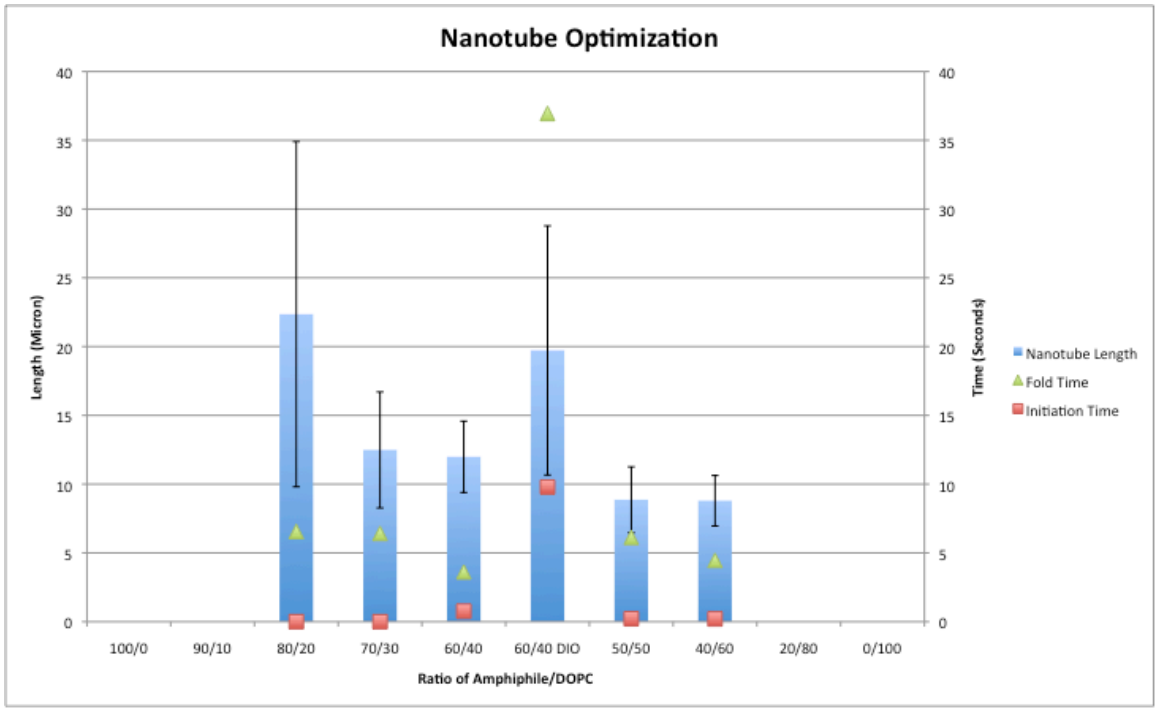

Chart S1. Optimization of amphiphile **1**/DOPC ratio in generation of high aspect ratio nanotubes, as measured by *wide field microscopy*. 60/40 was the selected ratio as the samples were replete with tubes of the most uniform length. Furthermore, disassembly initiation and folding times were the fastest. "60/40/DiO" indicates a 2:1:0.05 starting mixture in the presence of 0.05 equivalents of DiO. The initiation time for nanotube disassembly and folding time were both delayed in the presence of DiO, while observed tube length was increased.

5. Differential Scanning Calorimetry (DSC) Studies

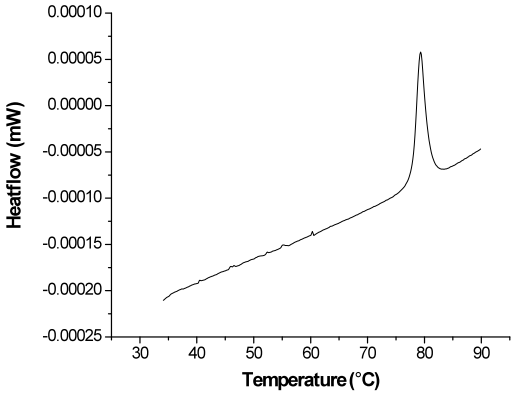

Figure S1. DSC scan of a 0.5 mg/ml solution of **1** in water between 30 and 90 °C.

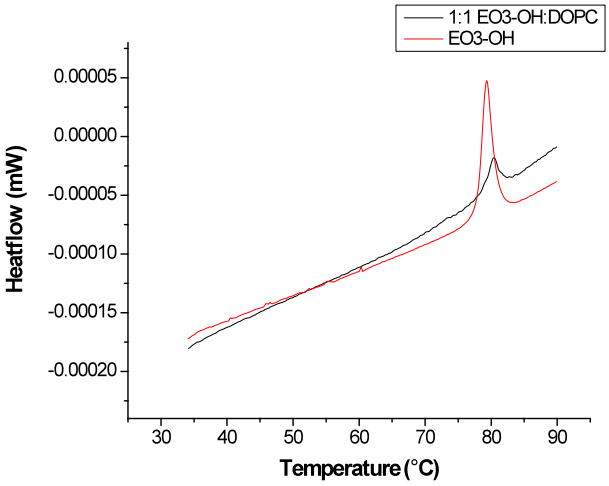

Figure S2. DSC scans of a 0.5 mg/ml solution of **1** in water (—) with a transition at 80 °C and 0.2 mg/ml of a 1:1 solution of 1/DOPC (1:1) in water (—) with a transition at 80 °C.

The phase behaviour of the nanotubes was studied using differential scanning calorimetry (DSC) to determine the level of phase separation between the amphiphile nanotube and the vesicle in order to establish to what extent DOPC might be incorporated within the nanotube bilayer. DSC measurements indicate a single phase transition at 80 °C with no difference observed in phase behaviour between nanotubes containing only

amphiphile and those obtained from a 2:1 amphiphile 1/DOPC solution (Supplementary Figure S2). This indicates that the DOPC and amphiphile **1** are essentially phase separated with the DOPC predominantly localized in the capping vesicles.

6. UV-Vis and IR spectra

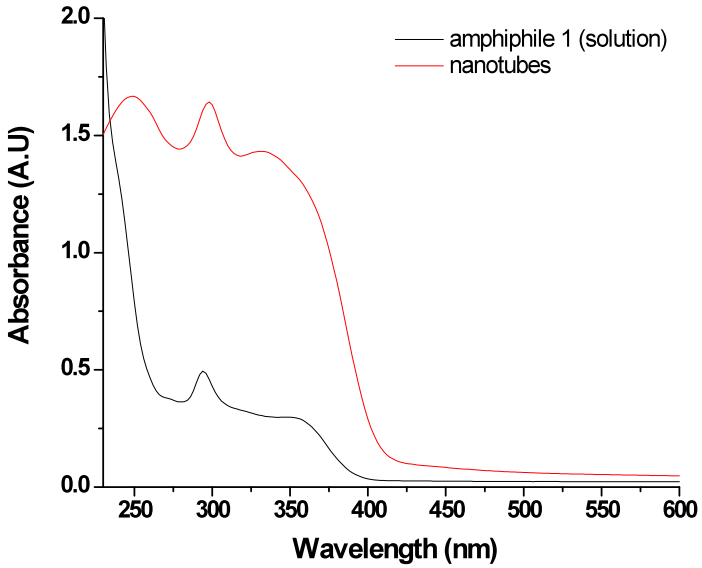

Figure S3 UV-Vis absorption spectra of amphiphile **1** in CH_2Cl_2 solution (2 x 10^{-5} M) (—) and diffuse reflectance spectrum of aqueous nanotube suspension (—)

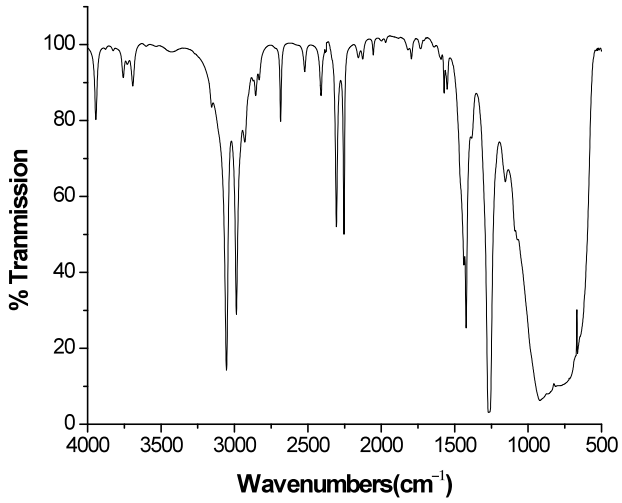

Figure S4 FT-IR spectrum (ATR) of amphiphile **1**

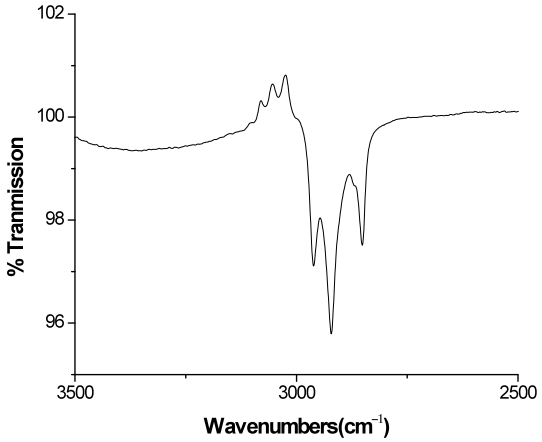

Figure S5 FT-IR spectrum (ATR) of nanotubes self-assembled from amphiphile **1**.

Infrared spectra of the nanotubes were taken from a dried layer of the nanotubes obtained by deposition of an aqueous suspension of the nanotubes onto the crystal of an ATR spectrometer. Infrared spectroscopy of the nanotubes show CH_2 stretching vibrations at 2960, 2921 and 2852 cm^{-1}, attributed to stretched alkyl chains in an interdigitated system[7] (see also reference 7).

7. Dye Inclusion and Transfer Studies

The amphiphilic green-fluorescent dye DiO (3,3′-dioctadecyloxacarbocyanine perchlorate) was added to a 2:1 amphiphile/DOPC mixture in water prior to tube formation. These dye-doped nanotubes were generated by combining (a) 50 μL of a 2 mg/mL amphiphile **1** solution in chloroform, (b) 10 μL of a 5 mg/mL DOPC solution in chloroform and (c) 1 μL of a 1 mg/mL DiO solution in chloroform. The solvent was removed to yield a thin film. This was then rehydrated with 250 μL double distilled water, sonicated and subjected to 5 freeze-thaw cycles to produce the desired nanotubes. Fluorescence microscopy images, with 505/470 nm excitation, show green fluorescent nanotubes, thereby confirming incorporation of DiO within the nanotubes.

Similarly, red-fluorescent DOPC vesicles (Figure S6) were generated with a 1:100 DiD/DOPC ratio. 250 μL of this 20 mg/mL (~5 mg) stock solution was taken and the solvent removed under vacuum. This was then rehydrated in 500 μL of 10 mM Hepes Buffer (pH 7.2) and sonicated. For preparation of the samples for microscopy studies, the DOPC vesicles were mixed with the nanotubes in a 1:1 ratio (10 μL of each aqueous solution). This solution was then diluted 100 times and imaged directly.

We further probed the potential mixing of the vesicle end caps and the tube core structure as amphiphile interchange between tubes and vesicles could be a useful mechanism for loading the tubes with cargo. Red-fluorescent DOPC vesicles were generated by incorporating the amphiphilic red-fluorescent dye 1,1′-dioctadecyl-3,3,3′,3′-tetramethylindodicarbocyanine (DiD). Since DiD is itself amphiphilic it is readily incorporated into the bilayer wall of the vesicles. Subsequent attachment of these vesicles to the nanotubes via the freeze-thaw method allows for the generation of red fluorescent nanotubes (Figure S6d). The red fluorescence is due to diffusion of DiD from the vesicle into the bilayer of the nanotube indicating that exchange between vesicle and tube does occur. Mixing the amphiphile **1** with green fluorescent dye 3,3′-dioctadecyloxacarbocyanine perchlorate (DiO) prior to tube formation results in intensely green fluorescent nanotubes (Figure S6b). Combination of these DiO labelled nanotubes

with DiD labelled DOPC vesicles results in capped nanotubes, in which the caps and tubes are both red and green fluorescent based on confocal microscopy images (Figures S6d-f). This is due to the amphiphilic character of the dye molecules involved, resulting in exchange between the bilayer compartments.

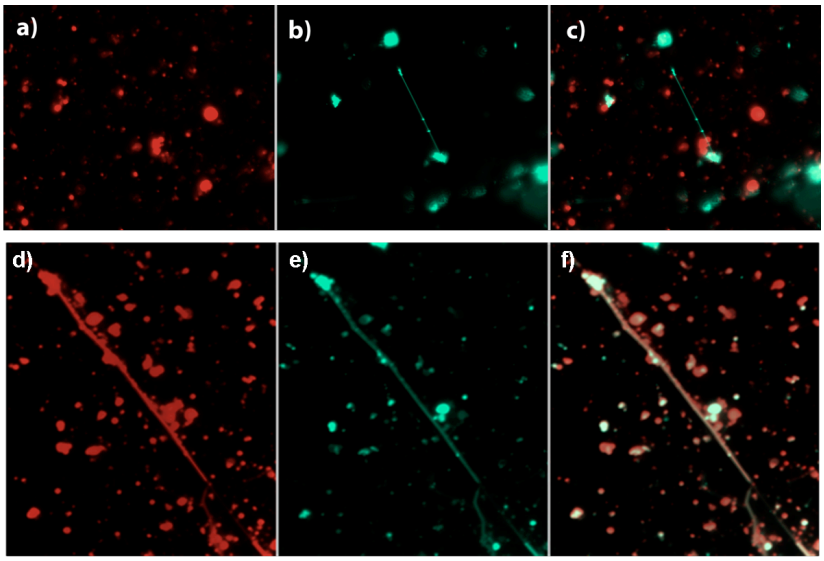

Figure S6. Confocal microscopy images of dye loaded vesicles and nanotubes. Prior to vesicle attachment to nanotube via freeze-thaw cycles: a) DiD loaded DOPC vesicles b) DiO loaded DOPC capped nanotubes, c) Overlay of images a) and b). d-f) After attachment of dye loaded DOPC vesicle to nanotube. d) red fluorescent vesicle capped nanotube, e) green fluorescent vesicle capped nanotube, e) overlay of red- and green emission channels of red and green fluorescent capped nanotube. Red fluorescence observed following 625 nm excitation and green fluorescence following 505/470 nm excitation.

8. Vesicle formation from pure cyclized amphiphile 2

Attempts to generate nanotubes from pure cyclized amphiphile **2** were unsuccessful even in the presence of a phospholipid. Cyclized amphiphile **2** was synthesised photochemically and used in both a 1:1 and 2:1 amphiphile/DOPC ratio as previously described for the *anti*-folded conformer. However, in all cases only vesicles were observed. Furthermore, pure cyclized amphiphile **2** in the absence of a phospholipid also only generates vesicles, with no evidence for nanotube formation observed.

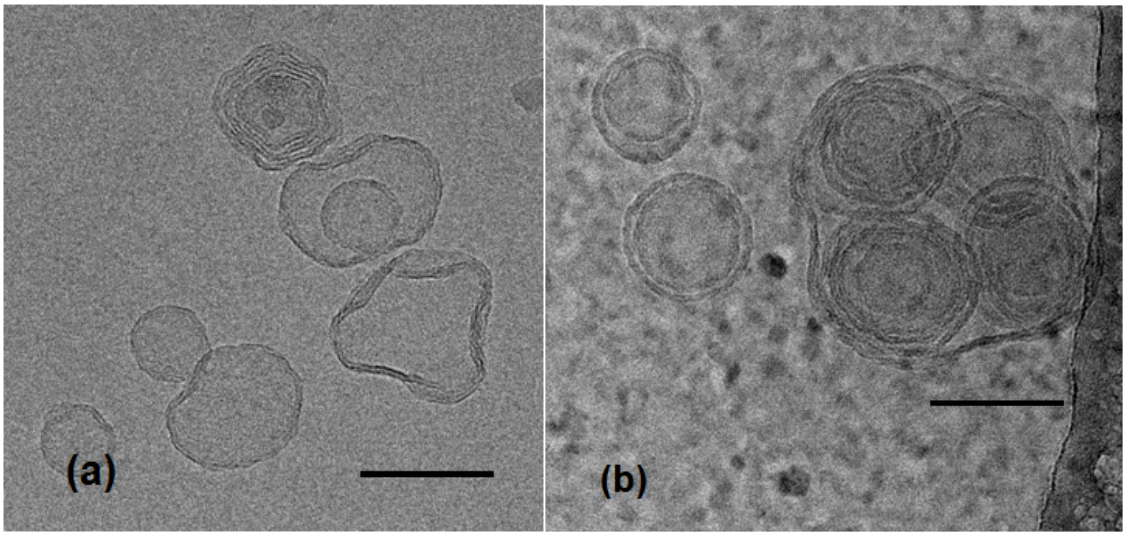

Figure S7. Vesicles generated from cyclized amphiphile **2** and DOPC (a) 2:1 amphiphile **2**:DOPC and (b) 1:1 amphiphile **2**:DOPC. Scale bar is 100 nm.

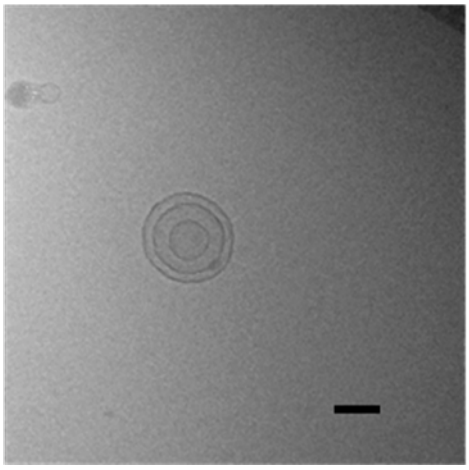

Figure S8. Vesicles generated from pure cyclized amphiphile **2**. Scale bar is 100 nm.

9. Spectral changes in nanotubes on irradiation at 400.8 nm.

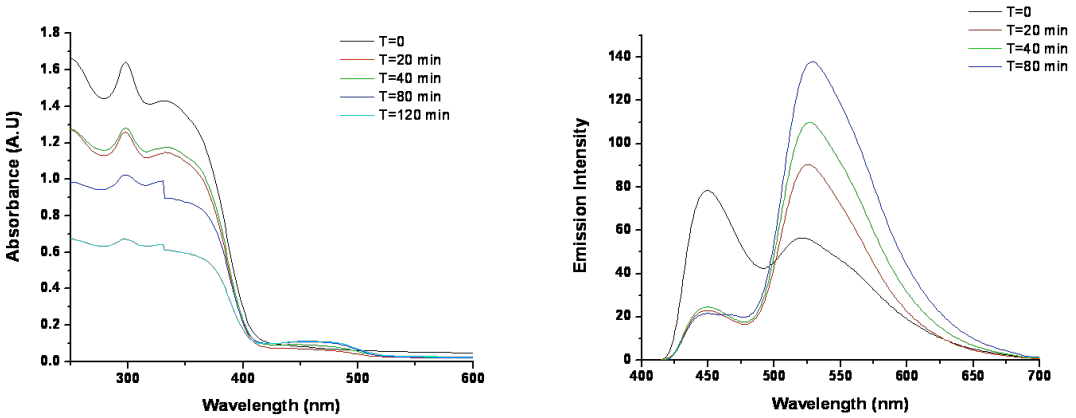

Figure S9. Changes in absorption and emission spectra of amphiphile nanotubes in water following 400.8 nm laser irradiation.

10. Description of Supplementary Movies

Movie S1: Epifluorescence microscopy of nanotubes composed of amphiphile **1** and DOPC (2:1) are irradiated with 488 nm wavelength of light followed by 390 nm wavelength of light from an LED source. We note that the initial irradiation causes no observable changes in the nanotube morphology while irradiation at a wavelength of 390 nm causes immediate disassembly leaving large aggregates.

Movie S1b: Duplicate experiment from Movie S1**.** Close-up of a single nanotube composed of amphiphile **1** and DOPC (2:1) using epifluorescence microscopy. Irradiation is from an LED source at a wavelength of 390 nm. Tube disassembly occurs within seconds and is complete in under a minute.

Movie S2: Confocal fluorescence microscopic images of nanotubes composed of amphiphile **1** and DOPC (2:1) are irradiated at 365 nm with a handheld UV lamp. We note that significant cyclization does not occur until after 45 seconds (green fluorescence) and then continues for several minutes. The result of the irradiation is small vesicle-like morphologies.

Movie S2b: Duplicate experiment from Movie S2. Confocal fluorescence microscopic images of nanotubes composed of amphiphile **1** and DOPC (2:1) irradiated at 365 nm with a handheld UV lamp. We note that the cyclization process is again slow, and the result of the irradiation is again small vesicle-like morphologies.

Movie S3: Epifluorescence microscopy imaging of long nanotubes composed of amphiphile **1**, DOPC, and DiO (2:1:0.05). Nanotubes are irradiated at 390 nm with an LED source. We note the responsive change in morphology is slower and distinctly different from the above results. The tubes can be seen coiling and curling to form a large aggregate.

Movie S3b: Duplicate experiment from Movie S3. Epifluorescence microscopy imaging of long nanotubes composed of amphiphile **1**, DOPC, and DiO (2:1:0.05) are irradiated with 390 nm with an LED source. We note the responsive change in morphology is slower (on the order of minutes) than that observed under the other conditions. The tubes can again be seen coiling and curling to form a large aggregate.

11. References

1. The structures were optimized with the AMBER force field. The PEG moieties were omitted from the calculations in benefit of the speed. The Hyperchem 7.5 software package was used. (HyperChem(TM) v. 7.5, Hypercube, Inc., 1115 NW 4th Street, Gainesville, Florida 32601, USA).

2. Tahara, Y. & Fujiyoshi, Y. A New Method to Measure Bilayer Thickness - Cryoelectron Microscopy of Frozen-Hydrated Liposomes and Image Simulation. *Micron.* **25**, 141-149 (1994).

3. Traikia, M., Warschawski, D. E., Recouvreur, M., Cartaud, J. & Devaux, P. F. Formation of unilamellar vesicles by repetitive freeze-thaw cycles: characterization by electron microscopy and P-31-nuclear magnetic resonance. *Eur. Biophys. J. Biophys. Lett.* **29**, 184-195 (2000).

4. Pollard, M. M. *et al*. Light-Driven Rotary Molecular Motors on Gold Nanoparticles. *Chem. -Eur. J.* **14**, 11610-11622 (2008).

5. Bouzide, A. & Sauve, G. Silver(I) oxide mediated highly selective monotosylation of symmetrical diols. Application to the synthesis of polysubstituted cyclic ethers. *Org. Lett.* **4**, 2329-2332 (2002).

6. Furrow, M. E. & Myers, A. G. Practical procedures for the preparation of N-tert-butyldimethylsilylhydrazones and their use in modified Wolff-Kishner reductions and in the synthesis of vinyl halides and gem-dihalides. *J. Am. Chem. Soc.* **126**, 5436-5445 (2004).

7. Hill, J. P. *et al*. Self-assembled hexa-peri-hexabenzocoronene graphitic nanotube. *Science.* **304**, 1481-1483 (2004).